The detector system for multi-nucleon transfer reaction study in GPSC of IUAC

*Mohit Kumar[1], A. Jhingan[1], Kavita Rani[2], N. Saneesh[1], Honey Arora[2], K. S. Golda[1], R. Ahuja[1], B. R. Behera[2], P. Sugathan[1]

[1]*Inter University Accelerator Centre, Aruna Asaf Ali Marg, New Delhi – 110067, INDIA*

[2]*Department of Physics, Panjab University, Chandigarh 160014, INDIA*

**email: mohit.kr.27@gmail.com*

Introduction

The study of multi-nucleon transfer has been a topic of interest to understand the fusion-fission dynamic near sub-barrier energies. The transfer channel effect has been studied with mass spectrometers and time of flight systems. In this paper, we proposed a hybrid system of time of flight (TOF) and energy measurement technique, which can also be utilized for measurement at forward angles and below/near the coulomb barrier energies. Old transfer field ionization chamber (IC) [1] was utilized with modification in MWPCs and charge sensitive preamplifers (CSPA). A new set of compact Hybrid detectors were developed to detect transfer product near to the beam axis. The setup was tested in offline as well as in-beam for the system ^{16}O + $^{144,154}Sm$ in the GPSC facility of IUAC.

Detector system

The system consists of two different configuration for below and above the Coulomb barrier energies. For the above barrier energies, The detector system consists of two position sensitive MWPCs, one fast timing MWPC and IC whereas for the below barrier, two set of Hybrid detectors are used instead of IC.

Ionization Chamber: The IC have been used for Z identification in transfer measurement experiments [2]. To improve the performance of the detector, a new set of 4 CSPA were fabricated and integrated with the anode inside the metallic housing of the IC, as shown in the Fig. 1(a). All the four segments of the anode provide the differential energy losses (ΔE) of the incident particles. The MWPC attached to the ionization chamber is a position sensitive counter in three electrode configuration (X-C-Y). The central timing frame and positions frame were prepared using 20 μm gold plated tungsten wires. The wires separation in the central and position frames were kept at a pitch of 0.3 mm and 0.63 mm respectively to enhance the timing signal's strength.

Hybrid detector: It is a combination of newly developed MWPCs and HYTAR detector [3]. The metallic body of MWPC was designed such that Hytar detector assembly can be attached to the back of MWPC. The Hybrid detector has a proportional region, an ionization region and a silicon PIPS detector in one assembly. as shown in Fig. 1(b). Full assembly provides timing, differential energy and total energy signals simultaneously. The compact design of these detectors allows them to use at extreme forward and backward angles.

Start MWPCs detectors: These are the transmission type fast timing MWPCs fabricated in three electrode geometry having an active area of (4 x 4) cm^2. To achieve the higher gain and fast decay time, 10 μm gold plated tungsten wire were used. The electrode assembly is mounted inside a metal housing and 0.5 μm thick Mylar foil was used to minimize the energy loss.

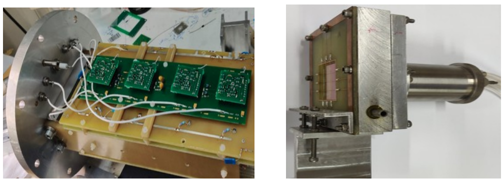

(a) (b)

Fig. 1 (a) Split anode ionization chamber with integrated CSPA units, (b) Hybrid detector system.

Performance test

Radioactive source test: The IC was tested off-line with ^{229}Th alpha source. The detector was operated at 90 mbar of isobutane pressure and detector biased at 990 V. The ΔE vs E spectrum is shown in the Fig. 2. All the five distinct peaks are well separated and an improvement of 25% in resolution was observed. The timing of MWPC were tested with fission source (^{252}Cf) at 2-3 mbar and 450 V. A rise time of ~2 ns was observed.

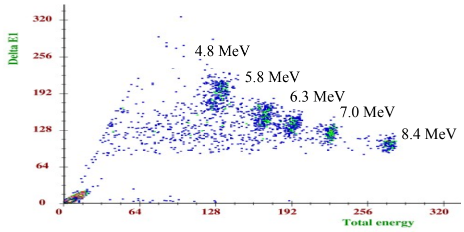

Fig. 2 Plot of ΔE vs E for alpha source (^{229}Th).

In-beam test: the detection system was setup for multi – nucleon transfer measurement in two steps, above and below barrier energies for the system ^{16}O +^{144,154}Sm at 72 MeV and 68 MeV respectively.

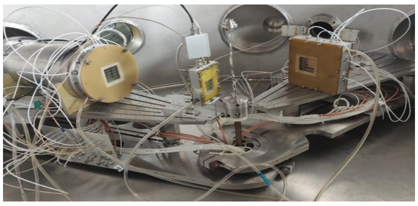

Fig. 3 Detector system for multi-nucleon transfer measurements above Coulomb barrier.

For 72 MeV (above barrier): One position sensitive MWPC with an active area of (4 x 2) inch was placed at a distance of 26.5 cm in one of the arm of GPSC to detect target-like transfer products in forward angle (3°-15°) whereas on the other arm at kinematically coincident angles, one start MWPC followed by IC separated by a distance of 29 cm were placed to detect projectile-like transfer products, the setup shown in Fig. 3. Absolute start-stop TOF parameter was collected, where master start taken from start MWPC and stop from the MWPC attached to the IC. IC provides differential energy loss parameters for Z separation. During the experiment, the MWPCs were operated at 6.5 mbar of isobutane gas pressure with cathode biased to 500 V. The IC was operated at 990 V, and a gas pressure of 90 mbar kept such that particles lose their 60 - 70 % of their energy within the first two anode segment. Timing signals were taken through home made fast timing preamplifer and differential energy loss through integrated CSPA. Fig. 4. Show the ΔE – E plot from IC. Here the differential energy loss from second anode segment is plotted against the total energy. 1 proton and 2 proton stripping channels are clearly separated.

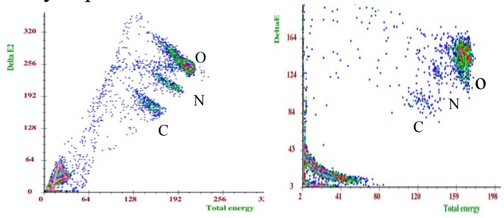

(a) (b)

Fig. 4 Plot (a) and (b) are showing ΔE vs E at 72 MeV and 68 MeV respectively.

Below the barrier (68 MeV): Two start MWPCs at an angle of 144° and 168° were placed on one arm and each followed by a hybrid detector at 41.5 cm and 33.5 cm from the start detector, setup shown in Fig. 5.

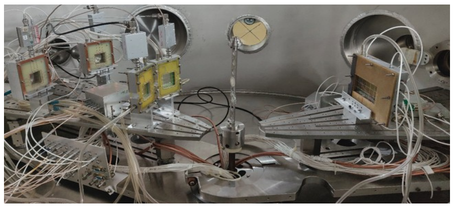

Fig. 5 Detector system for multi-nucleon transfer measurements below Coulomb barrier.

ΔE from Ionization chamber and E signal from silicon PIPS detector of the hybrid detector were collected for Z identification. The detectors were operated at 450 V and at 5.5 mbar of pressure. The effective count rate in this case was observed low due to lower transfer probability at these energy and also due to smaller active area (100 mm^2) of Si - PIPS detectors.

References

[1] A. Jhingan, *et al.* NIM A 745 (2014).
[2] Sunil Kalkal, *et al.* PRC 85 (2012).
[3] A. Jhingan, *et al.* NIM A 903,326(2018)